A Recursive Scheme for Computing Autocorrelation Functions of Decimated Complex Wavelet Subbands

Bart Goossens, Jan Aelterman, Aleksandra Pižurica, and Wilfried Philips

***Abstract*—This correspondence deals with the problem of the exact computation of the autocorrelation function of a real or complex discrete wavelet subband of a signal, when the autocorrelation function or alternatively the power spectral density (PSD) of the signal in the time domain (or spatial domain) is either known or estimated using a separate technique. The solution to this problem allows us to couple time domain noise estimation techniques to wavelet domain denoising algorithms, which is crucial for the development of "blind" wavelet-based denoising techniques. Specifically, we investigate the Dual-Tree complex wavelet transform (DT-CWT), which has a good directional selectivity in 2-D and 3-D, is approximately shift-invariant and yields better denoising results than a discrete wavelet transform (DWT). The proposed scheme gives an analytical relationship between the PSD of the input signal/image and the PSD of each individual real/complex wavelet subband which is very useful for future developments. We also show that a more general technique, that relies on Monte Carlo simulations, requires a large number of input samples for a reliable estimate, while the proposed technique does not suffer from this problem.**

***Index Terms*—Autocorrelation functions, complex wavelets.**

I. Introduction

Many noise estimation techniques, either designed for white or colored noise (e.g., [1]–[8]), estimate the noise power in the time (or spatial) domain, while this estimate is often used in a transformed domain, such as the wavelet domain [9]–[12]. An orthonormal linear transform preserves the noise variance of stationary white Gaussian noise. For nonorthogonal, overcomplete transforms or for colored noise, the situation is more complicated. Suppose that the covariance matrix of a finite length signal is given by $\mathbf{C}_x$ and the transform matrix is denoted as $\mathbf{W}$. The covariance matrix of the transformed signal $\tilde{x}$ becomes [13]

$$\mathbf{C}_{\tilde{x}} = \mathbf{W}\mathbf{C}_x\mathbf{W}^T. \tag{1}$$

Even though this relationship is simple, its computation is not, because the dimensions of the matrices can become very large, e.g., in 2-D or 3-D, which makes it impractical in realistic situations due to high memory and computational requirements. Also, if $\mathbf{C}_x$ is not known in advance and has to be estimated, a very large number of observations is required, which is also not feasible. Instead, it is common to assume weak-sense stationarity, which states that the correlation between two samples depends on their difference in position, but not on their absolute positions. This assumption significantly reduces the number of free parameters in $\mathbf{C}_x$ to be estimated, however the memory and computational requirements are still remaining.

For shift invariant transforms, such as the undecimated wavelet transform [13] or steerable pyramids [14], [15], the task of computing autocorrelation functions of subbands can be easily done by filtering and transforming a Dirac impulse to the transform domain and by computing the covariance matrix (or autocorrelation function) in each subband [11]. However, for shift *variant* transforms (such as the DWT [16], the DT-CWT [17] and the recently proposed Marr wavelet transform [18]), the obtained covariance matrix would depend on the exact position of the Dirac impulse, hence, the result would be incorrect.

A general approach would then be to use Monte Carlo simulations: first generate a noise signal with the known covariance matrix (or autocorrelation function), transform this noise signal to the wavelet domain and estimate the autocorrelation functions in each wavelet subband. This method is easy to implement, but has as major drawback that it suffers from estimation errors: often many input samples are needed to have a reliable estimate of the autocorrelation in each wavelet subband, as we will show in Section VI.

Despite the fact that recent efficient wavelet-based denoising techniques (e.g., [11], [19]) entirely rely on knowledge of the correlation properties of the transform coefficients, the computation and study of the autocorrelations has only received limited attention compared to the many papers that appeared on the topic of denoising. Averkamp and Houdré [20] analyze stationary second-order random processes in the DWT domain. Fowler [21] studies the variance of additive white noise, in nontight undecimated DWT frames. Chaux *et al.* [22], investigate noise covariance properties for dual-tree wavelet decompositions. Their analysis starts from the (cross)correlation functions between different continuous wavelet basis functions that have a closed form expression in frequency domain.

In this correspondence, we present an exact computation method for the autocorrelation functions in the real or complex wavelet domain, based on DSP theory, in a recursive manner similar to the Fast DWT scheme of Mallat based on iterated filter banks [13], with including decimations at every scale. This has the additional advantage that the computation is very fast and memory-friendly. Because our DSP approach directly uses the wavelet filter coefficients, we can also apply our technique in case of wavelets that do not have a closed form expression in frequency domain. We develop the expressions for the Dual-Tree Complex Wavelet transform (DT-CWT) [17], [23]. We have concentrated on the DT-CWT because of its popularity in signal and image processing. This transform is two times redundant in 1-D (four times in 2-D) and the coefficient magnitudes are approximately shift invariant, which yields significantly better results than a DWT for many real applications, e.g., denoising and usually better results than a nondecimated wavelet transform due to a better orientation selectivity. As such the derived expressions are important in a number of denoising methods. The method can also be easily extended to other types of multiresolution representations, based on similar derivations.

This correspondence is organized as follows: Section II introduces general concepts that are used in the remainder of this correspondence. In Section III the computation method for the 1-D DT-CWT is described. Next, extensions to the 2-D and higher dimensional oriented DT-CWT are presented, respectively, in Sections IV and V. Results and a discussion are given in Section VI. Finally, Section VII concludes this correspondence.

II. Preliminaries

In this section, we introduce some concepts that are used in the remainder of the correspondence. Let $F(z)$ denote the z-transform of a zero-mean signal $f(n) \in l_2(\mathbb{Z})$, i.e., $F(z) = \sum_{-\infty}^{+\infty} f(n)z^{-n}$. The discrete autocorrelation function of $f(n)$ is given by

$$r(n) = \mathrm{E}[f(m)\overline{f(n+m)}] \tag{2}$$

Manuscript received July 13, 2009; accepted March 04, 2010. Date of publication April 05, 2010; date of current version June 16, 2010. The associate editor coordinating the review of this manuscript and approving it for publication was Dr. Ivan W. Selesnick. The work of B. Goossens was supported by Special Research Fund (BOF) from Ghent University.

The authors are with the Department of Telecommunications and Information Processing (TELIN-IPI-IBBT), Ghent University, B-9000 Gent, Belgium (e-mail: Bart.Goossens@telin.UGent.be; Jan Aelterman@telin.ugent.be; Aleksandra.Pizurica@telin.UGent.be; Wilfried Philips@telin.UGent.be).

Digital Object Identifier 10.1109/TSP.2010.2047392

where $\overline{f(n)}$ denotes the complex conjugate of $f(n)$, and $\mathrm{E}[\cdot]$ is the mathematical expectation operator. In this correspondence, we assume that the signal is wide-sense stationary, such that $r(n)$ does not depend on m. The power spectral density (PSD) describes how the signal $f(n)$ is distributed in frequency. According to the Wiener-Khintchine Theorem (see, e.g., [24]), the PSD of $f(n)$ can be obtained through the discrete time Fourier-transform of the autocorrelation function $r(n)$

$$R(\omega) = \sum_{n=-\infty}^{\infty} r(n) e^{-j\omega n} \tag{3}$$

where ω is the frequency variable. To ease the notations, we will use the name PSD for the z-transform of $r(n)$ in the remainder of this correspondence, by defining $R(z) = \sum_{n=-\infty}^{\infty} r(n) z^{-n}$. The PSD in terms of the frequency variable ω can then be found by simply substituting $z = e^{j\omega}$.

Decimating the signal $f(n)$ by a factor 2 (without antialiasing filtering) leads to a signal $f'(n)$ with z-transform [25]

$$F'(z) = \frac{1}{2}\left(F\left(z^{\frac{1}{2}}\right) + F\left(-z^{\frac{1}{2}}\right)\right). \tag{4}$$

The autocorrelation function of the decimated signal $f'(n)$ is given by

$$r'(n) = \mathrm{E}[f'(m)\overline{f'(n+m)}] = r(2n).$$

Equivalently, in the z-domain, the PSD of the decimated signal $f'(n)$ can be obtained using

$$R'(z) = \frac{1}{2}\left(R\left(z^{\frac{1}{2}}\right) + R\left(-z^{\frac{1}{2}}\right)\right) \tag{5}$$

which means that the autocorrelation function of the decimated signal is equal to the decimated version of the autocorrelation function of the nondecimated signal. This is a crucial property for the further developments, as this will allow for an iterative scheme for computing autocorrelation functions after subsequent wavelet decompositions.

If we now consider two wide-sense stationary signals $f_1(n)$, $f_2(n)$ with z-transforms, respectively, $F_1(z)$ and $F_2(z)$, the cross-power spectrum (CPS) can be found as the z-transform of the corresponding cross-covariance function

$$S_{1,2}(z) = \sum_{n=-\infty}^{+\infty} \mathrm{E}[f_1(m)\overline{f_2(n+m)}] z^{-n}. \tag{6}$$

If the two signals are equal, $F_1(z) = F_2(z)$, the cross-power spectrum reduces to the PSD (3). Cross-power spectra are particularly useful when investigating the PSD of a signal that is a linear combination of a number of signals with known PSDs. For example, the signal $f_3(n) = af_1(n) + bf_2(n)$ has PSD

$$R_3(z) = |a|^2 R_1(z) + |b|^2 R_2(z) + a\bar{b}S_{1,2}(z) + \bar{a}b\overline{S_{1,2}(z)}. \tag{7}$$

We see that the PSD of $f_3(n)$ is influenced by the CPS between $f_1(n)$ and $f_2(n)$. This expression can be easily generalized to an arbitrary number of signals. Now, let $F_1'(z)$ and $F_2'(z)$ be decimated versions of respectively $F_1(z)$ and $F_2(z)$. The CPS between the decimated signals is again the decimated version of the CPS between both signals

$$S_{1,2}'(z) = \frac{1}{2}\left(S_{1,2}\left(z^{\frac{1}{2}}\right) + S_{1,2}\left(-z^{\frac{1}{2}}\right)\right). \tag{8}$$

Now that we have the relations for the PSD and the CPS before and after decimation, we can analyze how the autocorrelation of a signal changes through subsequent wavelet decompositions.

III. Autocorrelation in the 1-D DT-CWT Domain

The task we are facing is the computation of the autocorrelation functions for each scale of the DT-CWT transform, given an autocorrelation function of a signal in the time domain. The main idea of the proposed approach is to compute the autocorrelation iteratively, i.e., to express it as a function of the autocorrelation at the previous resolution level. Without loss of generality, we develop the expressions for one decomposition stage of the 1-D DT-CWT. Fig. 1 shows one stage of the dual tree WT, where two input signals with z-transforms $\tilde{F}_1(z)$ and $\tilde{F}_2(z)$ (and with PSDs $\tilde{R}_i(z) = \tilde{F}_i(z)\tilde{F}_i(z^{-1}), i = 1, 2$) are both lowpass and highpass filtered and subsequently subsampled. In the first stage of the wavelet transform, inputs of both trees are equal: $\tilde{F}_1(z) = \tilde{F}_2(z)$. For a multistage decomposition (not shown here), the process is iterated on the lowpass outputs $F_3(z)$ and $F_4(z)$ (i.e., $F_3(z)$ becomes $\tilde{F}_1(z)$ and $F_4(z)$ becomes $\tilde{F}_2(z)$). The filters $G_1(z)$ and $H_1(z)$ represent z-transforms of a conjugate quadrature filter (CQF) pair, $G_1(z)$ is an analysis wavelet filter and $H_1(z)$ is an analysis scaling filter. $G_2(z)$ and $H_2(z)$ denote the z transforms of a second CQF pair. Consequently the high pass filtered input signals have PSDs $\tilde{R}_i(z)G_i(z)G_i(z^{-1}), i = 1, 2$. Using (5), decimating the filtered signals by a factor 2 results in signals with PSDs $R_i(z), \quad i = 1, 2$, with

$$R_i(z^2) = \frac{1}{2}(\tilde{R}_i(z)G_i(z)G_i(z^{-1}) + \tilde{R}_i(-z)G_i(-z)G_i(-z^{-1})). \tag{9}$$

Similarly, for the lowpass outputs, we have $(i = 1, 2)$

$$R_{2+i}(z^2) = \frac{1}{2}(\tilde{R}_i(z)H_i(z)H_i(z^{-1}) + \tilde{R}_i(-z)H_i(-z)H_i(-z^{-1})). \tag{10}$$

Note that on the unit circle the filters are power complementary $|G_i(z)|^2 + |H_i(-z)|^2 = 2$, with $z = e^{j\omega}$ (see e.g., [16] and [25]). Because higher dimensional[1] complex wavelets are formed as tensor products of 1-D complex wavelets, some extra arithmetic is needed to compute the complex wavelet coefficients [23, eq. (7)]

$$F_1'(z) + jF_2'(z) = \frac{1}{\sqrt{2}}\begin{pmatrix} 1+j & 1-j \end{pmatrix}\begin{pmatrix} F_1(z) \\ F_2(z) \end{pmatrix} \tag{11}$$

which can be equivalently expressed as a linear transform to the vector $(F_1(z) \quad F_2(z))^T$

$$\begin{pmatrix} F_1'(z) \\ F_2'(z) \end{pmatrix} = \frac{1}{\sqrt{2}}\begin{pmatrix} 1 & 1 \\ 1 & -1 \end{pmatrix}\begin{pmatrix} F_1(z) \\ F_2(z) \end{pmatrix}. \tag{12}$$

By applying (7), $R_1'(z)$ and $R_2'(z)$, denoting, respectively, the PSDs of the real and imaginary parts of the complex wavelet coefficients $F_1'(z)$ and $F_2'(z)$, can be written as

$$\begin{aligned} R_1'(z) &= \frac{1}{2}(F_1(z)F_1(z^{-1}) + F_2(z)F_2(z^{-1}) + S_{1,2}(z) \\ &\quad + S_{1,2}(z^{-1})) \\ R_2'(z) &= \frac{1}{2}(F_1(z)F_1(z^{-1}) + F_2(z)F_2(z^{-1}) \\ &\quad - S_{1,2}(z) - S_{1,2}(z^{-1})) \end{aligned} \tag{13}$$

where $S_{1,2}(z)$ is the CPS between $F_1(z)$ and $F_2(z)$, that can be computed using (8)

$$\begin{aligned} S_{1,2}(z^2) = \frac{1}{2}(&\tilde{S}_{1,2}(z)G_1(z)G_2(z^{-1}) \\ &+ \tilde{S}_{1,2}(-z)G_1(-z)G_2(-z^{-1})) \end{aligned} \tag{14}$$

[1]In fact, this operation is not necessary in 1-D, but because it does not affect the PSDs of the complex wavelet magnitudes and because the phase modulation is used in higher dimensions, we explain this already for 1-D.

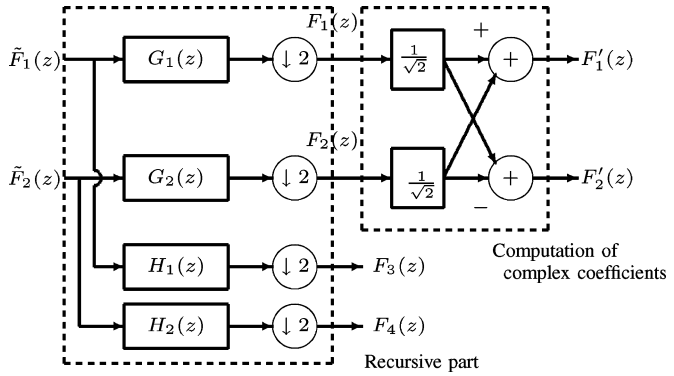

Fig. 1. Analysis building block of the 1-D DT-CWT (see text).

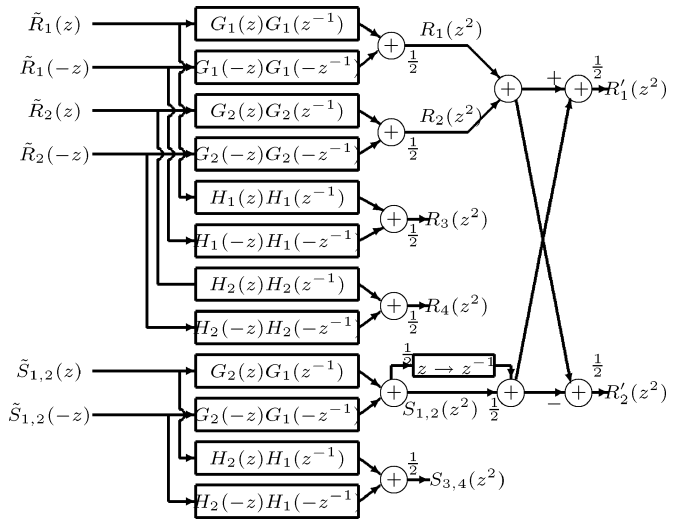

Fig. 2. Proposed computation scheme of the autocorrelation functions in the 1-D DT-CWT domain (one stage only). For multiple stages, this scheme is iterated on the outputs $R_3(z)$, $R_4(z)$ and $S_{3,4}(z)$. "$z \to z^{-1}$" denotes the operation that transforms $F(z)$ into $F(z^{-1})$ (i.e., time reversal).

with $\tilde{S}_{1,2}(z)$ the CPS between $\tilde{F}_1(z)$ and $\tilde{F}_2(z)$. The proposed scheme is summarized in Fig. 2.

In some applications, it may be necessary to have autocorrelation functions of the complex wavelet coefficients, instead of their real and imaginary parts. This can be achieved as follows.

$$R^{\mathrm{cplx}}(z) = (F_1'(z) + jF_2'(z))(F_1'(z^{-1}) - jF_2'(z^{-1})) \quad (15)$$

$$= R_1'(z) + R_2'(z) - jS_{1,2}'(z) + jS_{1,2}'(z^{-1}) \quad (16)$$

with the CPS between the real and imaginary parts of the coefficients given by

$$S_{1,2}'(z) = \frac{1}{2}(R_1(z) - R_2(z) - S_{1,2}(z) + S_{1,2}(z^{-1})). \quad (17)$$

In case one is only interested in the autocorrelation functions of the DWT (and not the DT-CWT), one can simply skip the computation of the complex coefficients in Fig. 1 and use $R_1(z)$ or $R_2(z)$ directly.

In a practical implementation, we wish to work directly with the wavelet filter coefficients instead of z-transfer functions, which relieves us from using symbolic algebra packages. First, we expand the input PSD and wavelet filters into polynomials in z: $G_i(z) = \sum_{n=-n_G}^{n_G} g_i(n)z^{-n}$, $H_i(z) = \sum_{n=-n_H}^{n_H} h_i(n)z^{-n}$, $\tilde{R}_i(z) = \sum_{n=-n_{\tilde{R}}}^{n_{\tilde{R}}} \tilde{r}_i(n)z^{-n}$ where $g_i(n)$, $h_i(n)$ and $\tilde{r}_i(n)$ denote the wavelet highpass filter coefficients, the lowpass coefficients and the autocorrelation function of the input signal, respectively, for tree i. Next, (9) and (10) are evaluated in the time domain by replacing the products by convolutions, based on the following z-transform properties:

$$H_i(z^{-1}) \leftrightarrow h_i(-n)$$
$$H_i(-z) \leftrightarrow (-1)^n h_i(n)$$
$$H_i(-z^{-1}) \leftrightarrow (-1)^n h_i(-n).$$

Subsequently, the cross-power spectrum between $F_1(z)$ and $F_2(z)$ (14) is computed using the same technique, in order to obtain the autocorrelation functions of the lowpass output signals $r_i(n)$, $i = 1, 2$, with $r_i(n)$ defined by $R_i(z) = \sum_{n=-n_R}^{n_R} r_i(n)z^{-n}$.

IV. Autocorrelation in the 2-D DT-CWT Domain

The reasoning from the previous section can be extended to the 2-D DT-CWT as follows: let $\tilde{F}_i(z_1, z_2)$ the z-transform of the input image of each tree ($i = 1, \ldots, 4$) and let $H_{i,m}(z_1, z_2)$ denote the corresponding separable wavelet filter where $m = 1, \ldots, 4$ respectively correspond to LL, LH, HL, and HH. Then the filtered and decimated subbands are given by

$$F_{i,m}\left(z_1^2, z_2^2\right) = \frac{1}{4}\sum_{k,l=0}^{1} H_{i,m}\left((-1)^k z_1, (-1)^l z_2\right) \cdot \tilde{F}_i((-1)^k z_1, (-1)^l z_2) \quad (18)$$

where the sum over k and l is due to the presence of aliasing terms by horizontal and vertical decimation. Equation (18) is in fact a 2-D extension of (4). The PSDs of these subbands are

$$R_{i,m}(z_1, z_2) = F_{i,m}(z_1, z_2)F_{i,m}\left(z_1^{-1}, z_2^{-1}\right) \quad (19)$$

and the cross-power spectra are computed as ($m = 2, 3, 4$)

$$S_{1,m}(z_1, z_2) = F_{1,m}(z_1, z_2)F_{4,m}\left(z_1^{-1}, z_2^{-1}\right)$$
$$S_{2,m}(z_1, z_2) = F_{2,m}(z_1, z_2)F_{3,m}\left(z_1^{-1}, z_2^{-1}\right). \quad (20)$$

By substituting (18) in (19) and (20), the PSDs $R_{i,m}(z_1, z_2)$, $i = 1, \ldots, 4, m = 1, \ldots, 4$, and $S_{b,m}(z_1, z_2)$, $b = 1, 2, m = 1, \ldots, 4$ can be directly written in terms of the PSDs of the input images of each tree ($\tilde{R}_{i,m}(z_1, z_2) = \tilde{F}_{i,m}(z_1, z_2)\tilde{F}_{i,m}(z_1^{-1}, z_2^{-1})$) and the cross-power spectra between the input bands $\tilde{S}_{1,m}(z_1, z_2)$, $\tilde{S}_{2,m}(z_1, z_2)$, with ($m = 1, \ldots, 4$)

$$\tilde{S}_{1,m}(z_1, z_2) = \tilde{F}_{1,m}(z_1, z_2)\tilde{F}_{4,m}\left(z_1^{-1}, z_2^{-1}\right)$$
$$\tilde{S}_{2,m}(z_1, z_2) = \tilde{F}_{2,m}(z_1, z_2)\tilde{F}_{3,m}\left(z_1^{-1}, z_2^{-1}\right). \quad (21)$$

Because of the linear phase modulation, the PSDs of the complex wavelet subbands are *not* equal to $\tilde{R}_{i,m}(z_1, z_2)$, but can be easily derived from the PSDs $\tilde{R}_{i,m}(z_1, z_2)$ by applying (13)

$$R_{1,m}'(z_1, z_2) = \frac{1}{2}\tilde{R}_{1,m}(z_1, z_2) + \frac{1}{2}\tilde{R}_{4,m}(z_1, z_2) + \frac{1}{2}\tilde{S}_{1,m}(z_1, z_2) + \frac{1}{2}\tilde{S}_{1,m}(z_1^{-1}, z_2^{-1})$$
$$R_{2,m}'(z_1, z_2) = \frac{1}{2}\tilde{R}_{2,m}(z_1, z_2) + \frac{1}{2}\tilde{R}_{3,m}(z_1, z_2) + \frac{1}{2}\tilde{S}_{2,m}(z_1, z_2) + \frac{1}{2}\tilde{S}_{2,m}(z_1^{-1}, z_2^{-1})$$

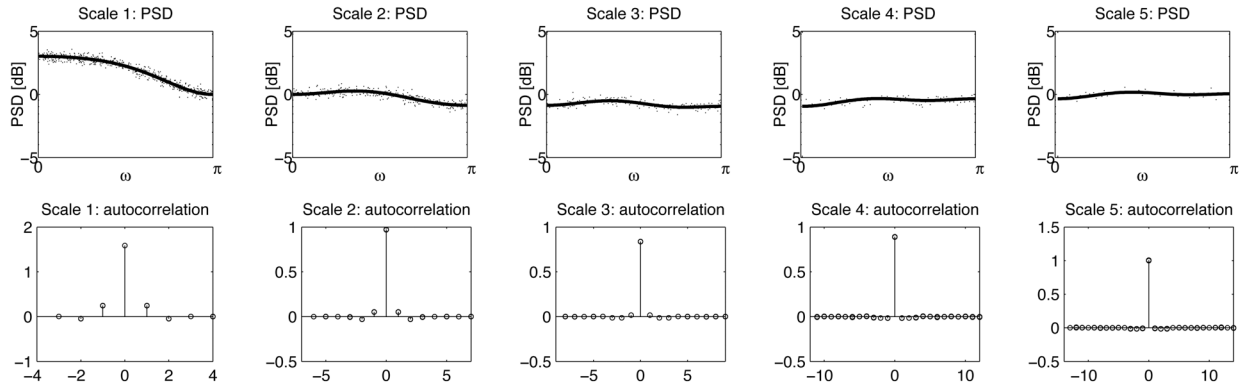

Fig. 3. Computed PSDs (top row) and autocorrelation functions (bottom row) for different subbands of the 1-D DT-CWT. The covariance function of the input signal is here a Dirac impulse. Dotted line (top row): estimated PSDs and autocorrelation functions using Monte Carlo simulations (see text), thick line: estimated PSDs and autocorrelation functions using the proposed scheme.

$$\begin{aligned} R'_{3,m}(z_1,z_2) &= \frac{1}{2}\tilde{R}_{2,m}(z_1,z_2)+\frac{1}{2}\tilde{R}_{3,m}(z_1,z_2) \\ &\quad -\frac{1}{2}\tilde{S}_{2,m}(z_1,z_2)-\frac{1}{2}\tilde{S}_{2,m}\left(z_1^{-1},z_2^{-1}\right) \\ R'_{4,m}(z_1,z_2) &= \frac{1}{2}\tilde{R}_{1,m}(z_1,z_2)+\frac{1}{2}\tilde{R}_{4,m}(z_1,z_2) \\ &\quad -\frac{1}{2}\tilde{S}_{1,m}(z_1,z_2)-\frac{1}{2}\tilde{S}_{1,m}\left(z_1^{-1},z_2^{-1}\right) \end{aligned} \quad (22)$$

with $m = 2,3,4$. Practically, the implementation does not pose any problems, because the wavelet filters in each tree of the transform are separable, which results in separability of the PSDs $\tilde{R}_{i,m}(z_1,z_2)$. Due to the linear phase modulations, the final PSDs $R'_{i,m}(z_1,z_2)$ are not separable, however they are a linear combination of separable functions.

V. Higher Dimensional Extensions

In the previous section, the computation scheme for the 2-D DT-CWT has been shown. For some applications (e.g., [26]), higher dimensional extensions are required. These extensions are straightforward, but quickly become very elaborate. For the sake of completeness we now present the extension to 3-D. We will consider one subband of tree $i = 1,2,\ldots,8$ and orientation $m = 2,3,4$ (LH, HL, and HH), with the corresponding separable wavelet filter $H_{i,m}(z_1,z_2,z_3)$. Calculations for the other subbands are analogous. Let $\tilde{F}_{i,m}(z_1,z_2,z_3)$ be the z-transform of the input wavelet band of each tree. The filtered and decimated subband is given by

$$\begin{aligned} &F_{i,m}\left(z_1^2,z_2^2,z_3^2\right) \\ &\quad=\frac{1}{8}\sum_{k,l,p=0}^{1} H_{i,m}((-1)^k z_1,(-1)^l z_2,(-1)^p z_3) \\ &\qquad \tilde{F}_{i,m}((-1)^k z_1,(-1)^l z_2,(-1)^p z_3). \end{aligned}$$

The PSD of this band is

$$R_{i,m}(z_1,z_2,z_3) = F_{i,m}(z_1,z_2,z_3)F_{i,m}\left(z_1^{-1},z_2^{-1},z_3^{-1}\right). \quad (23)$$

We want to know the PSDs of the real and imaginary parts of the complex coefficients of the DT-CWT, which involves linear transforms with transform matrix $\mathbf{A}$

$$\begin{pmatrix} F'_{1,m}(\mathbf{z}) \\ F'_{2,m}(\mathbf{z}) \\ F'_{3,m}(\mathbf{z}) \\ F'_{4,m}(\mathbf{z}) \\ F'_{5,m}(\mathbf{z}) \\ F'_{6,m}(\mathbf{z}) \\ F'_{7,m}(\mathbf{z}) \\ F'_{8,m}(\mathbf{z}) \end{pmatrix} = \underbrace{\frac{1}{2}\begin{pmatrix} 1 & 0 & 0 & -1 & 0 & -1 & -1 & 0 \\ 0 & 1 & 1 & 0 & 1 & 0 & 0 & -1 \\ 1 & 0 & 0 & 1 & 0 & 1 & -1 & 0 \\ 0 & -1 & 1 & 0 & 1 & 0 & 0 & 1 \\ 1 & 0 & 0 & 1 & 0 & -1 & 1 & 0 \\ 0 & 1 & -1 & 0 & 1 & 0 & 0 & 1 \\ 1 & 0 & 0 & -1 & 0 & 1 & 1 & 0 \\ 0 & -1 & -1 & 0 & 1 & 0 & 0 & -1 \end{pmatrix}}_{\mathbf{A}} \begin{pmatrix} F_{1,m}(\mathbf{z}) \\ F_{2,m}(\mathbf{z}) \\ F_{3,m}(\mathbf{z}) \\ F_{4,m}(\mathbf{z}) \\ F_{5,m}(\mathbf{z}) \\ F_{6,m}(\mathbf{z}) \\ F_{7,m}(\mathbf{z}) \\ F_{8,m}(\mathbf{z}) \end{pmatrix} \quad (24)$$

with $\vec{z} = [z_1,z_2,z_3]$. We also need the cross-power spectra

$$S_{i,m}(z_1,z_2,z_3) = F_{i,m}(z_1,z_2,z_3)F_{i,m}\left(z_1^{-1},z_2^{-1},z_3^{-1}\right) \quad (25)$$

in order to calculate the PSDs $R'_{i,m}(z_1,z_2,z_3)$

$$\begin{aligned} R'_{i,m}(z_1,z_2,z_3) = \frac{1}{4}\sum_{i''=1}^{8}\sum_{i'=1}^{8}[\mathbf{A}]_{i,i''}[\mathbf{A}]_{i,i'}, \\ F_{i',m}(z_1,z_2,z_3)F_{i'',m}\left(z_1^{-1},z_2^{-1},z_3^{-1}\right). \end{aligned}$$

These expressions contain 64 terms, of which 16 are nonzero. 4 of these 16 terms are the PSDs from (23), the other 12 terms are the cross-power spectra from (25).

VI. Results and Discussion

To compare our recursive scheme to general Monte Carlo (MC) simulations, we generate 256 input signals of length 4096 with a flat spectrum (i.e., the autocorrelation function in time domain is a Dirac pulse). For the MC simulations, the input signal is transformed to the complex wavelet domain, using the nearly symmetric Farras filters for 2-channel perfect reconstruction [27] in the first scale and the 6-tap Q-shift filters

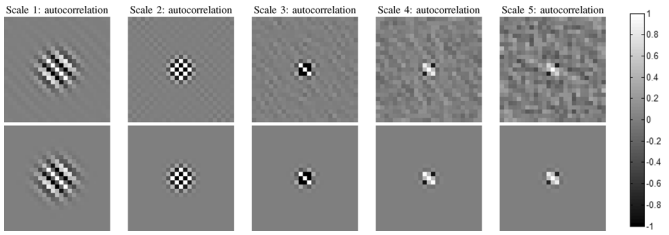

Fig. 4. Estimated (top row) and computed (bottom row) autocorrelation functions for different subbands (at orientation $-45°$) of the 2-D DT-CWT. The PSD of the input image is $F_1(z_1, z_2) = \sum_{m,n=-15}^{15} z_1^m z_2^n \exp(-(4/15)(m^2+n^2)) \cos(\pi(m+n))$. Gray corresponds to 0, white to positive correlations and black to negative correlations.

for the other scales [28]. Subsequently the autocorrelation functions are estimated in every wavelet subband. Finally, the estimated autocorrelation functions are averaged over all 256 signals to suppress the influence of estimation errors. For a fair comparison of our recursive scheme to the MC simulations, the same input samples and wavelet filters are used, without knowledge of the time-domain PSD. For the recursive scheme, we estimate the autocorrelation function of the input signal in time domain, using maximum likelihood estimation. Next, we compute the PSDs of the wavelet subbands using the recursive formulas presented in the previous Sections. In Fig. 3 the results are depicted for five scales of the DT-CWT. Only the autocorrelation functions and PSDs of the real parts of the complex wavelet coefficients are shown. For the technique employing MC simulations, statistical estimation errors are still significant (see the dashed lines in Fig. 3), while the proposed recursive scheme only starts from the time-domain estimation of the autocorrelation function of the input signal.

The reason for this difference in accuracy between both approaches lies in the decimation step in the DT-CWT procedure: this step makes the DT-CWT attractive for practical applications, as it greatly reduces memory and computational requirements by reducing redundancy. On the other hand, the decimation step reduces the number of available samples, which significantly lessens the estimation accuracy of the PSD as one progresses through different DT-CWT scales in the MC simulations. This seems to indicate loss of data, which is indeed the case if one looks at the DT-CWT bands separately. The loss of data is associated with subband aliasing (as all wavelet subbands suffer aliasing due to nonideal wavelet filters), which is nullified in the full DT-CWT framework, but not when operating on the subband separately. Our proposed method does not suffer the same ailment, as it is a closed form calculation from the autocorrelation function estimated in time domain.

The result also shows the nonorthogonality of the DT-CWT, as the input signal has a flat PSD while in the transform domain, the PSDs are not flat. Hence, a denoising algorithm that deals with white noise can not rely on the whiteness of the noise in the wavelet subbands. Some denoising algorithms in literature use the whiteness assumption: in this case the noise PSD in each complex wavelet subband is either over- or underestimated, resulting in oversmoothing and artifacts in the denoised images.

In Fig. 4, the experiment is repeated for the 2-D DT-CWT but for an oriented input autocorrelation function (for the exact definition see the caption of Fig. 4), again with an equal number of input samples for both methods. In the top row, the estimated autocorrelation functions using the general technique for one orientation of the 2-D DT-CWT are shown. For this task, a colored Gaussian noise image of size 1024×1024 was generated, according to the input autocorrelation function. In the bottom row, we show the autocorrelation functions computed using the proposed scheme. From Fig. 4 (top row), it can be seen that the autocorrelation functions estimated using the general Monte Carlo technique are quite noisy, especially for larger (coarse) scales. Obviously this is because the number of samples in each subband is too low to have a reliable estimation: in scale k this number given by $1024^2/4^k$, for the fifth scale this is 1024. As in 1-D, the influence of the noise can be reduced by generating multiple noise images and by averaging the estimated autocorrelation functions afterward.

More interestingly, the proposed scheme gives analytical relationships between the input PSD and the PSD of every complex wavelet subband. One other application could be to optimize the complex wavelet filter coefficients in a data-adaptive way, e.g., to enforce or have approximately white PSDs in the complex wavelet domain. (Approximate) uncorrelatedness of wavelet coefficients is advantageous for many applications, not only for denoising but also in image analysis, compression, etc.

VII. Conclusion

In this correspondence we have presented a recursive scheme for the computation of autocorrelation functions of complex wavelet subbands. This scheme is similar to the fast DWT of Mallat, but processes autocorrelation functions instead of raw signals or images. Using experiments, it is shown that time domain estimation of the autocorrelation function followed by the proposed recursive scheme yields more accurate results than Monte Carlo methods that directly estimate the autocorrelation functions of the wavelet subbands. The proposed scheme can be incorporated in recent wavelet denoising techniques (for developing "blind" restoration methods), moreover it also gives an analytical relationship between the PSD of the input signal/image and the PSD of each individual wavelet subband. This can be very useful for further developments of the DWT or DT-CWT, e.g., to optimize the filters in a data-adaptive way.

References

[1] S. I. Olsen, "Noise variance estimation in images," in *Proc. 8th SCIA*, Tromsø, Norway, May 25–28, 1993.
[2] S. I. Olsen, "Estimation of noise in images: An evaluation," *CVGIP: Graph. Models and Image Process.*, vol. 55, pp. 319–323, Jul. 1993.
[3] K. Rank, M. Lendi, and R. Ubenhauser, "Estimation of image noise variance," in *Proc. IEE, Vision, Image, Signal Process.*, 1999, vol. 146, pp. 80–84.
[4] A. De Stefano, P. R. White, and W. B. Collis, "Training methods for noise level estimation on wavelet components," *EURASIP J. Appl. Signal Process.*, vol. 16, pp. 2400–2407, 2004.
[5] B. C. Song and K. W. Chun, "Noise power estimation for effective denoising in a video encoder," in *Proc. IEEE Int. Conf. Acoust., Speech, Signal Process.*, Philadelphia, PA, 2005, pp. 357–360.
[6] A. Amer and E. Dubois, "Fast and reliable structure-oriented video noise estimation," *IEEE Trans. Circuits Syst. Video Technol.*, vol. 15, no. 1, pp. 113–118, 2005.
[7] V. Zlokolica, A. Pižurica, and W. Philips, "Noise estimation for video processing based on spatio-temporal gradient histograms," *IEEE Signal Process. Lett.*, vol. 13, pp. 337–340, Jun. 2006.
[8] C. Liu, W. T. Freeman, R. Szeliski, and S. B. Kang, "Noise estimation from a single image," in *IEEE Conf. Comput. Vision Pattern Recogn. (CVPR)*, 2006, pp. 901–908.
[9] S. E. Portilla J., "Adaptive wiener denoising using a Gaussian scale mixture model in the wavelet domain," in *Proc. IEEE Int. Conf. Image Process. (ICIP)*, 2001, vol. 2, pp. 37–40.
[10] L. Şendur and I. Selesnick, "Bivariate shrinkage with local variance estimation," *IEEE Signal Process. Lett.*, vol. 9, pp. 438–441, Dec. 2002.
[11] J. Portilla, V. Strela, M. Wainwright, and E. Simoncelli, "Image denoising using Gaussian scale mixtures in the wavelet domain," *IEEE Trans. Image Process.*, vol. 12, pp. 1338–1351, Nov. 2003.
[12] A. Pižurica and W. Philips, "Estimating the probability of the presence of a signal of interest in multiresolution single- and multiband image denoising," *IEEE Trans. Image Process.*, vol. 15, pp. 654–665, Mar. 2006.

[13] S. Mallat, "Multifrequency channel decomposition of images and wavelet models," *IEEE Trans. Acoust., Speech, Signal Process.*, vol. 37, pp. 2091–2110, Dec. 1989.
[14] W. T. Freeman and E. H. Adelson, "Design and use of steerable filters," *IEEE Trans. Pattern Anal. Mach. Intell.* , vol. 13, no. 9, pp. 891–906, 1991.
[15] E. P. Simoncelli and W. T. Freeman, "The steerable pyramid: A flexible architecture for multi-scale derivative computation," in *Proc. IEEE Int. Conf. Image Process.*, Wash., DC., Oct. 1995.
[16] I. Daubechies, *Ten Lectures on Wavelets*. Philadelphia, PA: Soc. Indust. Applied Math., 1992.
[17] N. G. Kingsbury, "Complex wavelets for shift invariant analysis and filtering of signals," *J. Appl. Computat. Harmon. Anal.*, vol. 10, pp. 234–253, May 2001.
[18] D. Van De Ville and M. Unser, "Complex wavelet bases, steerability, and the Marr-like pyramid," *IEEE Trans. Image Process.*, vol. 17, pp. 2063–2080, Nov. 2008.
[19] B. Goossens, A. Pižurica, and W. Philips, "Removal of correlated noise by modeling the signal of interest in the wavelet domain," *IEEE Trans. Image Process.*, vol. 18, no. 6, pp. 1153–1165, 2009.
[20] R. Averkamp and C. Houdré, "A note on the discrete wavelet transform of second-order processes," *IEEE Trans. Inf. Theory*, vol. 46, no. 4, pp. 1673–1676, 2000.
[21] J. E. Fowler, "The redundant discrete wavelet transform and additive noise," *IEEE Signal Process. Lett.*, vol. 12, no. 9, pp. 629–632, 2005.
[22] C. Chaux, J.-C. Pesquet, and L. Duval, "Noise covariance properties in dual-tree wavelet decompositions," *IEEE Trans. Inf. Theory*, vol. 53, pp. 4680–4700, Dec. 2007.
[23] I. W. Selesnick, R. G. Baraniuk, and N. G. Kingsbury, "The dual- tree complex wavelet transform," *IEEE Signal Process. Mag.* , vol. 22, pp. 123–151, Nov. 2005.
[24] H. Baher, *Analog and Digital Signal Processing.*. Chichester, U.K.: Wiley, 2001.
[25] M. Vetterli and C. Herley, "Wavelets and filter banks: Theory and design," *IEEE Trans. Signal Process.*, vol. 40, no. 9, pp. 2207–2232, 1992.
[26] J. Aelterman, B. Goossens, A. Pižurica, and W. Philips, "Removal of correlated Rician noise in magnetic resonance imaging," in *Proc. 16th Eur. Signal Process. Conf. (EUSIPCO)*, Aug. 2008.
[27] A. F. Abdelnour and I. W. Selesnick, "Design of 2-band orthogonal near-symmetric CQF," in *Proc. IEEE Int. Conf. Acoust., Speech, Signal Process.*, May 2001, pp. 3693–3696.
[28] N. G. Kingsbury, "Design of q-shift complex wavelets for image processing using frequency domain energy minimization," in *Proc. IEEE Int. Conf. Image Process.*, Barcelona, Sept. 15–17, 2003, pp. 1013–1016.

Linear Summation of Fractional-Order Matrices

Ran Tao, Feng Zhang, and Yue Wang

***Abstract*—Yeh and Pei presented a computation method for the discrete fractional Fourier transform (DFRFT) that the DFRFT of any order can be computed by a linear summation of DFRFTs with special orders. Based on their work, we investigate linear summation of fractional-order matrices in a general and comprehensive manner in this paper. We have found that for any diagonalizable periodic matrices, linear summation of fractional-order forms with special orders is related to the size and the period of the fractional-order matrix. Moreover, some properties and generalized results about linear summation of fractional-order matrices are also presented.**

***Index Terms*—Diagonalizable matrix, discrete fractional Fourier transform, eigendecomposition, fractional-order matrix.**

I. Introduction

Recently, the fractional Fourier transform (FRFT) has found many applications in signal processing and optics [1]–[3]. Besides being a generalization of the Fourier transform (FT), the FRFT can be interpreted as a rotation in the time-frequency plane and is related to other time-varying signal analysis tools [4], [5].

In order to digitally compute the FRFT, discrete counterpart of the FRFT, namely the discrete FRFT (DFRFT) has become an important issue in recent years. To date, several methods have been proposed for discretization of the FRFT. Among these methods, the DFRFT based on eigendecomposition of the DFT matrix $\mathbf{F}$ by using $\mathbf{F}$-commuting matrices has been found useful. Pei *et al.* first proposed the eigendecomposition-based definition of the DFRFT [6], and then Candan *et al.* consolidated this definition [7]. Hanna *et al.* considered generation eigenvectors of $\mathbf{F}$ by the singular value decomposition method and direct batch evaluation [8]–[10]. Some new $\mathbf{F}$-commuting matrices whose eigenvectors are better approximate the continuous Hermite–Gaussian functions are proposed in [11]–[13], and commuting matrices for other signal transforms are also investigated [14]–[18].

However, the computation cost of the eigendecomposition-based DFRFT is $O(N^2)$ and the DFRFT kernel needs recomputing while the order is changed. In [19], a new computation method for the eigendecomposition-based DFRFT is proposed. With this method, the DFRFT of any order (angle) can be computed by a linear combination of the DFRFTs with special orders. So, if the order of the DFRFT is changed, we only need compute the coefficients of the linear combination which can be obtained from an IDFT operation.

In fact, the new computation method for the DFRFT implies the idea of linear summation of multiple fractional-order matrices. In this paper, we investigate linear summation of fractional-order matrices in a general and comprehensive manner. We show that the result of linear summation of fractional-order matrices with special orders is determined by the relationship between the period and the size of the

Manuscript received July 26, 2009; accepted February 08, 2010. Date of publication February 25, 2010; date of current version June 16, 2010. The associate editor coordinating the review of this manuscript and approving it for publication was Prof. Ljubisa Stankovic. This work was supported in part by the National Science Foundation of China for Distinguished Young Scholars under Grant 60625104, the National Natural Science Foundation of China under Grants 60890070 and 60572094, and the National Key Basic Research Program Founded by MOST under Grant 2009CB724002 and 2010CB731902.

The authors are with the Department of Electronic Engineering, Beijing Institute of Technology, Beijing 100081, China (e-mail: rantao@bit.edu.cn; oUo@bit.edu.cn)

Digital Object Identifier 10.1109/TSP.2010.2044288